



Synthesis, investigation, spectroscopic characterization and computational modeling of mixed ligand complexes of Cu (II), Fe(II), Co(II) and Bi(V) using biological active streptomycin and oxime

Parashuram Mishra

Bioinorganic and Materials Chemistry Research Laboratory, Tribhuvan University, M.M.A.M. Campus, Biratnagar, Nepal.

ARTICLE INFO

Article history:

Received: 10 May 2012;

Received in revised form:

15 June 2012;

Accepted: 6 July 2012;

ABSTRACT

The novel ligand complexes of Cu(II), Fe(II), Co(II) and Bi(V) with biological active streptomycin and oxime were prepared and characterized by spectral techniques. The cell parameters were determined by X-ray powder pattern and the molecular models represent a better understanding of the arrangement of the atoms in the molecules in three dimensions.

© 2012 Elixir All rights reserved.

Keywords

Oxime,
Streptomycin,
Metal complexes,
Antibiotics,
XRPD.

Introduction

An intensive member of studies on the formation of mixed ligand complexes using antibiotic reveals a realization of their importance particularly in their role in biological process[1]. The formation of mixed ligand chelates is a general feature of systems where a metal is present with two or more ligands. The study of these complexes shows that their formations are a favored process over that of simple complexes [2]. The study of these type of complexes involving hydroxyl groups as the primary ligand oxime and biomolecule secondary ligand of streptomycin serve as useful models for gaining a better understanding of hydroxyl –metal ion – substrate complexes, which play an important role in metallo-hydroxyl complexes.[3,4] With the aim to continue the exploration of the coordination mode adopted by the novel ligand which has been performed a preparative and structural work by using the novel ligand some d-block metal ions and p-block metal by employing the hydroxyl oxygen antibiotic drug biomolecules[4-10] with deprotonated of group in coordinate manner of streptomycin and oxime. The solid chelates are characterized by using different physico-chemical methods like IR, UV-Vis, and XRD powder pattern is also utilized as a confirmatory tool for elucidation the cell parameters along with structure were optimized with Chem Office Ultra-12 programme.

Experimental details

All the chemicals used were obtained from Aldrich Chemical Company, USA and used as received.

Synthesis of complexes:

A hot solution of metal chloride (1mmol, 20ml) in 80% methanol (20ml) was added to another solution of ligand and was mixed in 100ml round bottom flask. The mixture was refluxed for several hours at a temperature of 75°C. The mixture was cooled at room temperature and the precipitate was filtered

and washed with 50% methanol and dried at room temperature too[11].

Physical measurements

Elemental C, H, and N analyses were carried out on a Carlo-Erba 1106 elemental analyzer. Molar conductance was measured on an ELICO conductivity bridge (type CM82T). Infrared spectra were recorded on Perkin Elmer 137 instruments as KBr pellets. Electronic spectra of the three solid complexes were recorded in DMSO-d₆ solution on a Shimadzu UV mini-1240 spectrophotometer. ¹H NMR spectra of the ligand and its complexes were recorded on Bruker Advance 300 spectrophotometer at 100 kHz modulation and higher frequency. Electron impact mass spectra were recorded on JEOL, JMS, and DX-303 mass spectrometer.

Results and Discussions

Satisfactory results of elemental analysis (Table 1) and spectral studies revealed that the complexes were of good purity. Various attempts to obtain the single crystals have so far been unsuccessful. X-ray diffraction studies indicate crystalline nature of the metal complexes. The complexes were soluble in polar solvents.

Vibrational Spectra

Novel ligand exhibits absorptions 1122, 1660, 2538 cm⁻¹. These bands are very metal complexes indicating non – involvement of the oxygen atoms of hydroxyl group in coordination with the metal ions[12]. The stretching frequencies of ligand hydroxyl and give bands at 3268 and 3522 cm⁻¹ with a shoulder at about 3550 cm⁻¹. These bands appear in the complexes as strong band absorption in the region 3420 - 3445 cm⁻¹. These bands appear for the new complex at the same wave number, ruling out the participation of hydroxyl oxygen in the coordination. These results confirm that complexation occurred and suggest that the oxygen of the hydroxyl group is involved in the coordination sphere [13]. The vibrational bands due to

rocking & wagging modes of water and metal – oxygen stretching modes are observed in the 825 – 350 cm^{-1} region for all the complexes may be attributed to coordinated water[14]. This can be confirmed with the help of thermo grams. A new band in the 600 – 300 cm^{-1} regions in the spectra of the complexes is assignable to $\nu(\text{M} - \text{O})$.

¹H NMR

The ¹H NMR spectra of the streptomycin complexes of Cu(II), Fe(II), Co(IV) and Bi(V) in a DMSO-*d*₆ solvent of the ligand and M-ligand complex show well-resolved signals. Figure 4: ¹H NMR spectrum of complex (I). The N-H protons of amine, which would have undergone very rapid exchange with the solvent, appear as quite broad ragged doublet around 3.56 (ppm) and 3.67 (ppm) coordinated with metals(II) which disappeared in the metal complex spectra. In complex 3, peaks range 1.22-1.75 ppm are from coordinated water. The various assignments of ¹H NMR of the complexes are summarized in table 3. Chemical shift are in ppm from TMS & multiplicity in parentheses (bd, broad; d, doublet; m, multiplet).

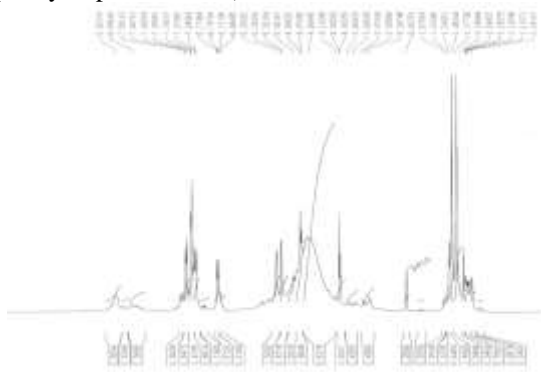


Figure 1. ¹H NMR of the novel ligand

Electronic spectra measurements

The electronic absorption spectra of the free ligands in water solvent three confirming coordination of the ligands to metal, in addition to appearance of new bands maxima at 278 nm, 217 nm and 204 nm in legand 1 which have their origin in the $\pi \rightarrow \pi^*$ and $n \rightarrow \pi^*$ transition within the organic ligand. The Bi(IV) complex 1 show 345 nm and 295 nm in UV range due to charge transfer while in complex 2 367 nm, 348 nm 277 nm strong absorption due to charge transfer and the high –energy band at 276 nm is assigned to a charge-transfer, metal \rightarrow ligand or vice versa.

TOF–MS spectra

Mass spectrometry has been successfully used to investigate molecular species $[\text{MH}]^+$ in solution [15]. The molecular ion peaks of the ligands and complexes have been used to confirm the proposed formula. The pattern of the mass spectrum gives an impression of the successive degradation of the target compound with the series of peaks corresponding to the various fragments. Their intensity gives an idea of stability of fragments. The ligand starts degradation and finally forms $[\text{C}_{23}\text{H}_{25}\text{NO}_7]^+$, 427/428 (100 % m/z values). In the TOF–mass spectra of metal complexes initial fragmentation pattern is again similar (loss of two water molecules), a mononuclear nature for these complexes $[\text{M}(\text{L})]^+$ can be deduced. The fragmentation of complexes as m/z: 822.25 (100.0%), 824.24 (44.6%), 823.25 (33.6%), 825.25 (16.2%), 824.25 (9.3%), 826.25 (3.9%), 823.24 (3.0%), 825.24 (1.3%) for complex 1, m/z: 815.25 (100.0%), 816.25 (37.7%), 817.26 (8.6%), 813.26 (6.4%), 817.25 (2.2%), 814.26 (2.1%), 818.26 (1.8%), 816.26 (1.2%) for complex 2, m/z: 818.25 (100.0%), 819.25 (36.0%), 820.26 (5.5%), 820.25 (4.1%),

821.26 (1.6%) for complex 3 and m/z: 968.30 (100.0%), 969.30 (33.6%), 970.30 (9.3%), 969.29 (3.0%), 971.30 (1.3%) for complex 4.

Kinetics of thermal decomposition

Recently, there has been increasing interest in determining the rate- dependent parameters of solid-state non- isothermal decomposition reactions by analysis of TG curves. Thermogravimetric (TG) and differential thermo gravimetric (DTA) analyses were carried out for different metal–streptomycin complexes in ambient conditions. The thermogravimetric analysis revealed that the complexes of Cu & Fe loses mass between 65°C and 140°C, corresponding to nearly 15 % of the total mass, followed by considerable decomposition up to 600°C, which corresponds to the decomposition of the ligand molecule leaving metal oxide (FeO & Bi_2O_3 , respectively) as residue. The complexes of Co & Bi decomposes nearly 10% of the total mass up to temperature 170°C, followed by considerable decomposition of the ligand molecule up to 650°C, leaving metal oxide (CuO and FeO respectively) as residue. On the basis of thermal decomposition, the kinetic analysis parameters such as activation energy (E^*), enthalpy of activation (ΔH^*), entropy of activation (ΔS^*), free energy change of decomposition (ΔG^*) were evaluated graphically by employing the Coats – Redfern relation

$\text{Log} [-\text{Log} (1 - \alpha) / T^2] = \text{log} [AR / \theta E^*(1 - 2RT/E^*)] - E^*/2.303RT$
Where α is the mass loss up to the temperature T, R is the gas constant, E^* is the activation energy in J mole^{-1} , θ is the linear heating rate and the term $(1 - 2RT/E^*) \cong 1$. A straight line plot of left hand side of the equation (1) against $1/T$ gives the value of E^* while its intercept corresponds to A (Arrhenius constant). The Coats and Redfern linearization plots, confirms the first order kinetics for the decomposition process. The calculated values of thermodynamic activation parameters for the decomposition steps of the metal complexes are reported in Table 4. According to the kinetic data obtained from the TG curves, the activation energy relates the thermal stability of the metal complexes. Among metal complexes, activation energy increases as complex 3 ~ complex 2 < complex 4 < complex 1, same trends happens with thermal stability of metal complexes. All the complexes have negative entropy, which indicates that the complexes are formed spontaneously. The negative value of entropy also indicates a more ordered activated state that may be possible through the chemisorptions of oxygen and other decomposition products. The negative values of the entropies of activation are compensated by the values of the enthalpies of activation, leading to almost the same values for the free energy of activation.

X-ray powder diffraction studies

In absence of single crystal, x-ray powder data is especially useful to deduce accurate cell parameters. The diffraction pattern reveals the crystalline nature of the complex. The indexing procedure were performed using (CCP4, UK) Crysfire programme [19] giving different crystal system with varying space group. The merit of fitness and particle size of the metal complexes has been calculated (Figure.) spectra of complexes. The cell dimensions of the complexes are shown in table 5.

3D - Molecular modeling

3D molecular modeling of the proposed structure of the complexes was performed using CsChem3D Ultra -11 program package. The correct stereochemistry was assured through the manipulation and modification of the molecular coordinates to obtain reasonable low energy molecular geometries. The

optimized structures of the complexes were performed by MM2 programme contained CS chem. Office programme. The potential energy of the molecule was the sum of the following terms: $E = E_{str} + E_{ang} + E_{tor} + E_{vdw} + E_{oop} + E_{ele}$. Where all E 's represent the energy values corresponding to the given types of interaction. The subscripts str, ang, tor, vdw, oop and ele denote bond stretching, angle bonding, torsion deformation, van der waals interactions, out of plain bending and electronic interaction, respectively. The Cu is coordinated with tetrahedral with ligand, Fe and Co-ligand are coordinated with octahedral while Bi(V) coordinated with ligand in trigonal pyramidal structure.

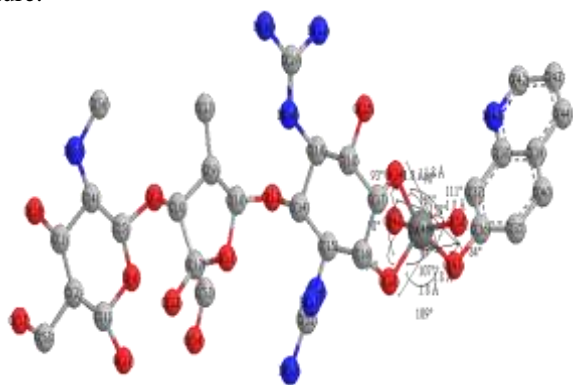


Figure 2. Optimized structure of Cu-Ligand(Complex1)with energy 65.667 Kj/m0l

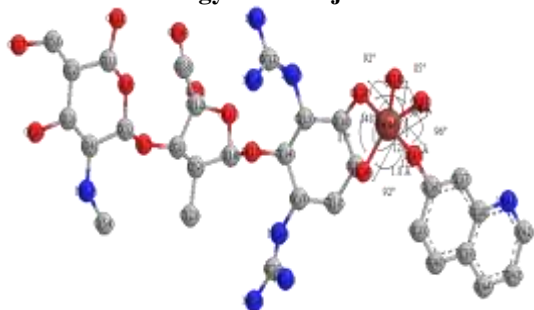


Figure 3. Optimised structure of Fe-ligand (Complex 2) with energy 49.9352 Kj/m0l

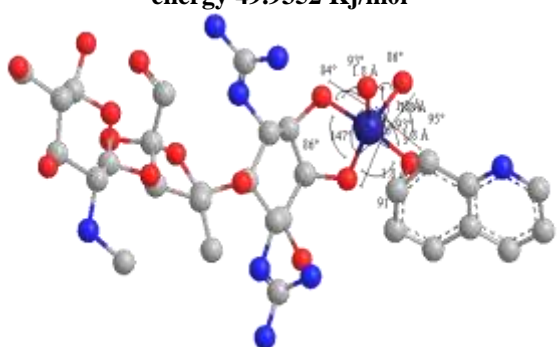


Figure 4. Optimised structure of Co-ligand(Complex 3) with energy 66.667 Kj/m0l

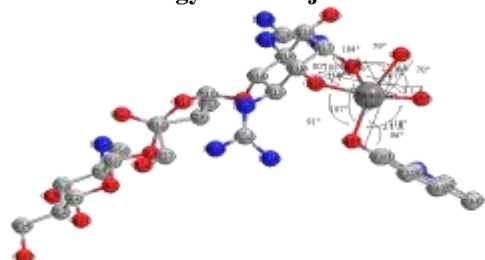


Figure 5. Optimised structure of Bi -ligand(Complex 4) with energy 116.667 Kj/m0l

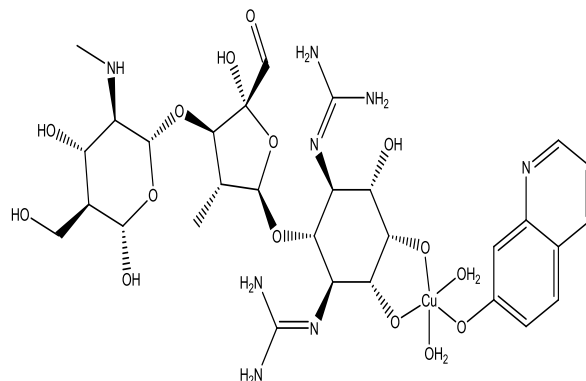


Figure 6. Asymmetry structure of complex 1.

Conclusions

The most important feature of novel ligand which have an organic frame work and which have been a lot of nitrogenous – containing primary or secondary amino groups with oxygen from hydroxyl groups is their binding ability. These atoms formed new bonds with different metals. The binding abilities of the metals were determined by different spectral techniques. To find out the crystal lattice parameters, particle size were calculated and density of the crystal were determined by Archimedes principle. The molecular structures of the complexes were proposed with help of Chem Office Ultra-11 programe. The Metal –organic frame work complexes will be ailment of anti- cancer.

References

- Jian-Guo Cui, Lei Fan, Li-Liang Huang, Hong-Li Liu, Ai-Min Zhou, Synthesis and evaluation of some steroidal oximes as cytotoxic agents: Structure/activity studies, *Steroids*, 74, Issue 1, 2009,62-7
- Gábor Orgován, Béla Noszál, NMR analysis and site-specific protonation constants of streptomycin, *Journal of Pharmaceutical and Biomedical Analysis*, 59, 2012, 78-82.
- Jianguo Cui, Lei Fan, Yanmin Huang, Yi Xin, Aimin Zhou, Synthesis and evaluation of some steroidal oximes as cytotoxic agents: Structure/activity studies (II), *Steroids*, Volume 74, Issue 12, 4 November 2009, Pages 989-995.
- Natalija M. Krstić, Mira S. Bjelaković, Željko Žizak, Mirjana D. Pavlović, Zorica D. Juranić, Vladimir D. Pavlović, Synthesis of some steroidal oximes, lactams, thiolactams and their antitumor activities, *Steroids*, Volume 72, Issue 5, May 2007, Pages 406-414.
- Yuanbin Xie, Yanling Liu, Chi Ma, Zhongmin Yuan, Wenya Wang, Zhenyu Zhu, Guoquan Gao, Xianguo Liu, Hengxin Yuan, Ruzhu Chen, Shoujian Huang, Xuelan Wang, Xiaonan Zhu, Xuemin Wang, Zixu Mao, Mingtao Li, Indirubin-3'-oxime inhibits c-Jun NH₂-terminal kinase: anti-apoptotic effect in cerebellar granule neurons, *Neuroscience Letters*, Volume 367, Issue 3, 9 September 2004, Pages 355-359
- Georg Surkau, Konrad J. Böhm, Klaus Müller, Helge Prinz, Synthesis, antiproliferative activity and inhibition of tubulin polymerization by anthracenone-based oxime derivatives, *European Journal of Medicinal Chemistry*, Volume 45, Issue 8, August 2010, Pages 3354-3364.
- Pankaj Makadia, Shailesh R. Shah, Harikishore Pingali, Pandurang Zaware, Darshit Patel, Suresh Pola, Baban Thube, Priyanka Priyadarshini, Dinesh Suthar, Maanan Shah, Suresh Giri, Chitrang Trivedi, Mukul Jain, Pankaj Patel, Rajesh Bahekar, Effect of structurally constrained oxime-ether linker on PPAR subtype selectivity: Discovery of a novel and potent series of PPAR-pan agonists, *Bioorganic & Medicinal*

Chemistry, Volume 19, Issue 2, 15 January 2011, Pages 771-782.

8. Timothy W. Failes, Andrew R. Battle, Catherine Chen, Carleen Cullinane, Ross Woods, Robyn Elliott, Glen B. Deacon, Trevor W. Hambley, Structural and anticancer properties of hydrogen bonded diphenylphosphate adducts of Pt(IV) complexes: The importance of pK_a matching, J.Inorganicbiochemistry, In Press, Accepted Manuscript, Available online 27 April 2012.

9. Nathalia Villa dos Santos, Adriana F. Silva, Vani Xavier Oliveira Jr., Paula Homem-de-Mello, Giselle Cerchiaro, Copper(II) complexation to 1-octarepeat peptide from a prion protein: Insights from theoretical and experimental UV-visible studie, J.Inorganicbiochemistry, In Press, Accepted Manuscript, Available online 27 April 2012.

10. Verónica Paredes-García, Ricardo C. Santana, Rosa Madrid, Bianca Baldo, Andrés Vega, Evgenia Spodine, Single Crystal Electron Paramagnetic Resonance Spectra of Cu^{II} ions in Cu(tyrosine)₂: A Study of Weak Exchange Interactions mediated by Resonance Assisted Hydrogen Bonds (RAHB), J.Inorganic Biochemistry, In Press, Accepted Manuscript, Available online 27 April 2012.

11. Tânia S. Morais, Tiago J.L. Silva, Fernanda Marques, M. Paula Robalo, Fernando Avecilla, Paulo J. Amorim Madeira, Paulo J.G. Mendes, Isabel Santos, M. Helena Garcia, Synthesis of organometallic ruthenium(II) complexes with strong activity against several human cancer cell lines, J.Inorganic

Biochemistry, In Press, Accepted Manuscript, Available online 27 April 2012.

12. Tiziana Pivetta, Francesco Isaia, Gaetano Verani, Carla Cannas, Laura Serra, Carlo Castellano, Francesco Demartin, Federica Pilla, Matteo Manca, Alessandra Pani, Mixed-1,10-phenanthroline-Cu(II) complexes: Synthesis, cytotoxic activity versus hematological and solid tumor cells and complex formation equilibria with glutathione, J.Inorganic Biochemistry, In Press, Accepted Manuscript, Available online 27 April 2012.

13. Paramasivam Jaividhya, Rajkumar Dhivya, Mohamad Abdulkadhar Akbarsha, Mallayan Palaniandavar, Efficient DNA Cleavage Mediated by Mononuclear Mixed Ligand Copper(II) Phenolate Complexes: The Role of Co-ligand Planarity on DNA Binding and Cleavage and Anticancer Activity, J.Inorganic Biochemistry In Press, Accepted Manuscript, Available online 8 May 2012.

14. Lok Yung Chan, Hoi Hin Kwok, Renee Wan Yi Chan, Malik Joseph Sriyal Peiris, Nai Ki Mak, Ricky Ngok Shun Wong, Michael Chi Wai Chan, Patrick Ying Kit Yue, Dual functions of ginsenosides in protecting human endothelial cells against influenza H9N2-induced inflammation and apoptosis, *Journal of Ethnopharmacology*, 137, 3, 11 2011, 1542-1546.

15. Ann M. Dring, Linnea E. Anderson, Saima Qamar, Matthew A. Stoner, Rational quantitative structure-activity relationship (RQSAR) screen for PXR and CAR isoform-specific nuclear receptor ligands, *Chemico-Biological Interactions*, 188, 3, 2010, 512-525.

Table 1
Color, reaction yield and elemental analysis of

Complex	Empirical formula	Color	Yield (%)	Analysis: found (calculated) (%)				M.Pt. °C
				C	H	N	M	
Cu(L) Complex (1)	C ₃₀ H ₄₈ N ₈ O ₁₅ Cu	Blue	70	43.77 (43.65)	5.76 (5.87)	13.61 (13.57)	7.77 (7.57)	65.25
[Fe(L) Complex(2)	C ₃₀ H ₄₈ N ₈ O ₁₅ Fe	greenish	75	44.18 (44.12)	5.81 (5.84)	13.74 (13.36)	6.85 (6.81)	71.25
Co(L)H ₂ O Complex(3)	C ₃₀ H ₄₈ N ₈ O ₁₅ Co	Pinkish	80	44.29 (44.65)	5.78 (5.67)	13.15 (13.12)	28.17 28.18	65.36
Bi(L) Complex(4)	C ₃₀ H ₄₈ N ₈ O ₁₅ Bi	White	65	37.20 (36.27)	4.87 (4.87)	11.29 (11.16)	21.17 (24.91)	90.32

Table 2. Assignment of IR spectral data (cm⁻¹) of the metal complexes

Frequency	OH	OH	OH	NH ₂	NH ₂	M-O
C ₃₀ H ₄₈ N ₈ O ₁₅ Cu	3425(s,b)	1633(s)	1528(s)	1236(m)	690(s)	425(m)
C ₃₀ H ₄₈ N ₈ O ₁₅ Fe	3427(s,b)	1636(m)	1525(s)	1227(m)	685(s)	450(s)
C ₃₀ H ₄₈ N ₈ O ₁₅ Co	3460	1639(m)	1503(m)	1218(w)	686(s)	428(m)
C ₃₀ H ₄₈ N ₈ O ₁₅ Bi	3356(s,b)	1640(m)	1469(s)	1224(w)	696(s)	429(s)

Table 3. ¹H N M R data of free novel ligands and their complexes

Compounds	δ (ppm)
C ₃₀ H ₄₆ N ₈ O ₁₃	[3.35(s)1H,OH],16.77(s)1H,OH,16.77(s),1H,OH,3.65(m),5H,OH,2.0(s)1H,NH,7.16(s)1H,NH ₂ 3.83(m)1H,CH,8.19(d)1H,CH(Ar),9.00(s)1H,CH(Ar),8.62(m) 1H,CH(Ar),7.78(s)1H,CH(Ar),2.52---3.98(m)4H,(m)CH,3.98--- 4.73(d),2H,CH,1.35(s) 3H,CH ₃ 1.06(s)6H,CH ₃]
Complex 1	8.17(bd)1H 3.26(m)2H, 1.95(bd),2.05,1.94(d)6.54(d),104,4.45(m),3.76(m)0,6.12(d),
Complex 2	8.12(bd)8.17(bd)1H3.26(m)2H, 1.95(bd),2.05,1.94(d)6.54(d),104,4.555(m),3.76(m)0,6.13(d),
complex 3	8.18(bd)1H3.26(m)2H, .85(bd),2.05,1.74(d)6.54(d).1.04(m),4.45(m),3.76(m)0,6.12(d),

Table 4. Thermodynamic activation parameters of the metal complexes

Complex	Order/n	Steps	E*/Jmol ⁻¹	A/sec ⁻¹	ΔS*/JK ⁻¹ mol ⁻¹	ΔH*/Jmol ⁻¹	ΔG*/kJmol ⁻¹	k×10 ² s ⁻¹
C ₃₀ H ₄₈ N ₈ O ₁₅ Cu	1	I	57.66	1.125×10 ⁵	-92.49	112.745	61.228	1.72
		II	65.804	1.256×10 ⁵	-110.175	96.114	89.18	1.02
C ₃₀ H ₄₈ N ₈ O ₁₅ ZFe	1	I	59.066	6.27×10 ⁵	-85.136	74.10	55.29	3.27
		II	7.178	1.16×10 ⁵	-109.603	125.89	93.104	1.79
C ₃₀ H ₄₄ N ₈ O ₁₃ Co	1	I	56.35	1.4501×10 ⁵	-67.345	118.76	44.135	1.45
		II	65.08	1.171×10 ⁴	-75.96	54.691	74.96	1.14
C ₃₀ H ₄₄ N ₈ O ₁₃ Bi	1	I	59.59	2.28×10 ⁶	-55.01	70.98	36.566	1.01
		II	67.88	1.53×10 ⁶	-80.731	28.16	80.547	0.611

Table 5. Crystallographic data of complexes

Compounds	Complex 1	Complex 2	Complex 3	Complex 4
Formula	C ₃₀ H ₄₈ N ₈ O ₁₅ Cu	C ₃₀ H ₄₈ N ₈ O ₁₅ Fe	C ₃₀ H ₄₈ N ₈ O ₁₅ Co	C ₃₀ H ₄₈ N ₈ O ₁₅ Bi
FW	823.28	815.25	818.25	968.72
Temp (K)	293	293	293	293
Wavelength	1.54056	1.54056	1.54056	1.54056
Crystal System	Triclinic	Monoclinic	Monoclinic	Monoclinic
Space group	P-1	IMNA	P 2/m	P2/m
Unit cell dimension				
a(Å)	5.9118	10.312	9.575	10.312
b(Å)	11.1885	7.7972	7.553	7.7972
c(Å)	17.6895	8.9554	8.959	8.9554
α°	117.5208	90.00	90.00	90.00
β°	122.1025	120.9166	112.00	120.00
γ°	54.15113	90.00	90.00	90.00
Volume (Å ³)	783.78	1617.78	598.23	617.78
θ range (°)	21.696-75.106	13.811-61.987	10-65	12-67
Limiting indices	0 ≤ h ≤ 5 0 ≤ k ≤ 6 0 ≤ l ≤ 2	-6 ≤ h ≤ 5 0 ≤ k ≤ 6 0 ≤ l ≤ 4	-10 ≤ h ≤ 5 0 ≤ k ≤ 1 0 ≤ l ≤ 4	-1 ≤ h ≤ 2 -4 ≤ k ≤ 4 0 ≤ l ≤ 7
Particle size(nm)	10.922	81.82	56.99	11.92
Intensity (%)	7.2-100	5.9-100	4.5-100	3.4-100
R indices	0.0000156	0.0000615	0.0000754	0.0000362
Density	1.07405	1.7437	1.034	1.151
Z	2	2	1	1

Table 6. selected bond length and bond angles

Bond lengths		Bond angles	
Complex 1		Complex 1	
O(50)-Cu(46)	1.8496	O(50)-Cu(46)-O(47)	159.3361
O(47)-Cu(46)	1.8423	O(50)-Cu(46)-O(24)	90.0898
O(24)-Cu(46)	1.8161	O(50)-Cu(46)-O(45)	84.0974
O(45)-Cu(46)	1.8159	O(50)-Cu(46)-O(28)	106.8067
O(28)-Cu(46)	1.8143	O(47)-Cu(46)-O(24)	92.7689
		O(47)-Cu(46)-O(45)	86.6935
		O(47)-Cu(46)-O(28)	93.6808
		O(24)-Cu(46)-O(45)	161.2147
		O(24)-Cu(46)-O(28)	89.6146
		O(45)-Cu(46)-O(28)	109.1636
		Cu(46)-O(45)-C(36)	111.3466
Complex 2		Complex 2	
O(50)-Fe(46)	1.8249	O(50)-Fe(46)-O(47)	85.0352
O(47)-Fe(46)	1.8254	O(50)-Fe(46)-O(24)	147.5420
O(24)-Fe(46)	1.8130	O(50)-Fe(46)-O(45)	86.3886
O(45)-Fe(46)	1.8158	O(50)-Fe(46)-O(28)	92.4108
O(28)-Fe(46)	1.8170	O(47)-Fe(46)-O(24)	127.2650
		O(47)-Fe(46)-O(45)	95.9064
		O(47)-Fe(46)-O(28)	86.1679
		O(24)-Fe(46)-O(45)	92.4740
		O(24)-Fe(46)-O(28)	87.3604
		O(45)-Fe(46)-O(28)	177.4995
		Fe(46)-O(45)-C(36)	111.8175
Complex 3		Complex 3	
O(50)-Co(46)	1.8398	O(50)-Co(46)-O(47)	86.4842
O(47)-Co(46)	1.8375	O(50)-Co(46)-O(24)	147.0588
O(24)-Co(46)	1.8038	O(50)-Co(46)-O(45)	93.1012
O(45)-Co(46)	1.8132	O(50)-Co(46)-O(28)	84.4861
O(28)-Co(46)	1.8082	O(47)-Co(46)-O(24)	125.5749
Complex 4		Complex 4	
O(50)-Bi(46)	2.1229	O(47)-Co(46)-O(45)	95.4856
O(47)-Bi(46)	2.1232	O(47)-Co(46)-O(28)	93.0793
O(24)-Bi(46)	2.1010	O(24)-Co(46)-O(45)	91.1820
O(45)-Bi(46)	2.1012	O(24)-Co(46)-O(28)	86.2063
O(28)-Bi(46)	2.1017	O(45)-Co(46)-O(28)	170.9457
		Complex 4	
		O(50)-Bi(46)-O(47)	69.8798
		O(50)-Bi(46)-O(24)	79.0970
		O(50)-Bi(46)-O(45)	164.3778
		O(50)-Bi(46)-O(28)	104.1443
		O(47)-Bi(46)-O(24)	86.9842
		O(47)-Bi(46)-O(45)	95.5461
		O(47)-Bi(46)-O(28)	166.8467
		O(24)-Bi(46)-O(45)	106.5010
		O(24)-Bi(46)-O(28)	80.2881
		O(45)-Bi(46)-O(28)	91.2677
		Bi(46)-O(45)-C(36)	109.6305
		Bi(46)-O(28)-C(16)	110.1838
		Bi(46)-O(24)-C(17)	108.3688